Dielectric properties of lithium niobate–tantalate crystals

D. Xue, K. Betzler*, H. Hesse

Fachbereich Physik, Universität Osnabrück, D-49069 Osnabrück, Germany

Abstract

Dielectric properties, including linear (refractive index) and second-order nonlinear optical responses, of $LiNb_{1-y}Ta_yO_3$-type mixed single crystals with $y = 0.00$, 0.81, 0.92, 0.97, and 1.00 have been quantitatively studied. Based on the corresponding crystal compositions, the chemical bond method was applied. The results show that the dielectric susceptibilities at 1.064 μm decrease remarkably with increasing tantalum content in the mixed-crystal system lithium niobate–tantalate. © 2000 Elsevier Science Ltd. All rights reserved.

Keywords: A. Insulators; C. Crystal structure and symmetry; D. Optical properties

1. Introduction

Mixed ferroelectrics have been the focus of intensive fundamental and applied research for many years. Interest in the study of these materials arises from the fact that the physical properties of crystalline materials are governed to a large extent by the composition of the crystals, thus can be tuned by varying the composition. One of the simplest systems of ferroelectric mixed crystals is lithium niobate–tantalate (LNT) as both end members exhibit the same crystal structure (space group $R3c$) with only slight differences in the lattice and positional parameters. Both border components which make up the system, lithium niobate $LiNbO_3$ (LN) and lithium tantalate $LiTaO_3$ (LT), belong to the small group of ferroelectric materials, which are important for applications in many technological fields.

Lithium niobate is of great interest since several decades for both fundamental sciences and applications in optics due to its large electrooptical and nonlinear optical (NLO) coefficients [1,2]. Its crystal structure [3,4] and defect structure [5,6] have attracted considerable interest these years. Recent improvements have been achieved in the field of holographic storage where two-color [7] and two-center redording [8] have been developed. In the field of frequency conversion, wavelength range and conversion efficiency could be greatly extended using periodically

poled structures in bulk crystals [9,10] or in combination with waveguides [11].

Lithium tantalate has gained interest in similar fields due to its large NLO coefficients [12] and photorefractive damage resistance [13]. Applications include surface acoustic wave devices [14], holographic storage [15,16], channel waveguides [17,18], periodically poled structures [19], and electro-optic deflectors [20].

Despite all similarities, there are also specific differences of the physical properties, which make it important to study the mixed system LNT in more detail. Phase matching properties, e.g. for NLO applications like sum frequency generation or optical parametric oscillation could be influenced very sensitively by the composition. To a certain degree, the mixed system yields also a simple crystal modeling method that may lead to good functional materials.

As lithium niobate has been much more intensively investigated than lithium tantalate, it is reasonable to use lithium niobate as the starting point in the considerations of the current mixed system.

Lithium niobate is a slightly nonstoichiometric, typically Li-deficient crystal, preferably grown at the congruently melting composition with 48.5 mol% Li_2O. A large variety of dopants ranging from the +1 valent state H^+ to the +3 valent state earth cations can be introduced into the crystal structure frame of lithium niobate crystals. Most are known to occupy Li sites [21]. This can be understood from the defect structure of Li-deficient lithium niobate, all recent investigations have shown that preferably

---

* Corresponding author. Fax: +49-541-969-3512.

E-mail address: klaus-betzler@uni-osnabrueck.de (K. Betzler).

Table 1
Calculated dielectric susceptibilities of $LiNb_{1-y}Ta_yO_3$ mixed crystals at 1.064 μm

	$LiNb_{1-y}Ta_yO_3$				
	$y = 0.00$	$y = 0.81$	$y = 0.92$	$y = 0.97$	$y = 1.00$
Refractive index n_0	2.23	2.077	2.056	2.046	2.04
d_{22} (pm/V)	2.72	1.84	1.72	1.67	1.64
d_{31} (pm/V)	−4.94	−3.15	−2.91	−2.79	−2.73
d_{33} (pm/V)	−25.31	−17.80	−16.78	−16.32	−16.03

lithium vacancies are formed [5,6]. From the viewpoint of the synthetic chemistry, the dopant usually prefers to occupy the vacant lattice site in the host. Even excess Nb in nonstoichiometric lithium niobate occupies vacant Li sites.

In contrast to these Li-site dopants, tantalum is isomorphous to niobium and replaces niobium when introduced into the crystal structure frame of lithium niobate. As tantalum can substitute for niobium up to 100%, i.e. up to a complete exchange, it is very important to study the influence of the tantalum 'dopant' on the properties of lithium niobate crystals. Any changes in the crystal composition will finally affect all physical properties of the crystal, such as the linear dielectric response, i.e. the refractive index, and the second-order NLO susceptibility. Our previous experimental and theoretical studies have shown the important effect of different compositions of lithium niobate on its corresponding dielectric responses, respectively [22,23], but both studies explain the effect of niobium cations on lithium sites in lithium niobate crystals on the dielectric responses. Therefore, the current study about the tantalum dopant on niobium sites will, in a sense, complement our earlier work towards a more thorough understanding of the influence of different dopants, occupying different lattice sites, on the dielectric properties of lithium niobate type crystals. Eventually general information can be gained about the way how dielectric properties can be effectively modified.

Our chemical bond method allows us to understand dielectric responses of crystal materials from corresponding crystallographic structures by using the constructed structure–property relationship [24]. In an earlier work [25], we have quantitatively studied linear and second-order NLO responses (at 1.064 μm) of LN and LT, from their respective detailed crystallographic structures at room temperature. Since LT and LN have the similar crystallographic structures, we therefore, in the present work, can do some predictions of dielectric responses of the mixed lithium niobate–tantalum crystals, $LiNb_{1-y}Ta_yO_3$ with $y = 0.00, 0.81, 0.92, 0.97$, and 1.00 (hereafter, abbreviated as LNT). In the present work, their dielectric responses include refractive indices n_0 at 1.064 μm and all independent second-order NLO tensor coefficients d_{22}, d_{31}, and d_{33} at 1.064 μm.

2. Theoretical method

As shown in the previous studies [24], the chemical bond method regards certain macroscopic physical properties of a crystal as the combination of the contributions of all constituent chemical bonds. According to the relationship between the crystal structure and dielectric responses of crystal materials, the linear and second-order NLO properties of any crystal can be calculated using the appropriate geometric sum of the respective properties of its corresponding constituent chemical bonds. On the basis of the crystallographic structure of an assigned crystal, its linear and second-order NLO susceptibilities χ and d_{ij} thus can be written as:

$$\chi = \sum_{\mu} F^{\mu} \chi^{\mu} = \sum_{\mu} N_b^{\mu} \chi_b^{\mu} \tag{1}$$

and

$$d_{ij} = \sum_{\mu} \left\{ \frac{G_{ij}^{\mu} N_b^{\mu} (0.5) \{ [(Z_A^{\mu})^* + n(Z_B^{\mu})^*] / [(Z_A^{\mu})^* - n(Z_B^{\mu})^*] \} f_i^{\mu} (\chi_b^{\mu})^2}{d^{\mu} q^{\mu}} \right.$$
$$\left. + \frac{G_{ij}^{\mu} N_b^{\mu} s(2s-1) [r_0^{\mu} / (r_0^{\mu} - r_c^{\mu})]^2 f_c^{\mu} (\chi_b^{\mu})^2 \rho^{\mu}}{d^{\mu} q^{\mu}} \right\}, \tag{2}$$

respectively. Parameters used in Eqs. (1) and (2) and in Table 1 include:

F^{μ}: Fraction of bonds of type μ composing the crystal;
χ^{μ}: Linear susceptibility contribution from μ-type bonds;
N_b^{μ}: Number of bonds of type μ per cm³;
χ_b^{μ}: Susceptibility of a single bond of type μ;
G_{ij}^{μ}: Geometrical contribution of chemical bonds of type μ;
$(Z_A^{\mu})^*$, $(Z_B^{\mu})^*$: Effective number of valence electrons of A and B ions, respectively;
n: Ratio of numbers of two elements B and A in the bond valence equation [23];
f_i^{μ}, f_c^{μ}: Fractions of ionic and covalent characteristics of the individual bonds, $f_i^{\mu} = (C^{\mu})^2 / [(E_h^{\mu})^2 + (C^{\mu})^2]$ and $f_c^{\mu} = 1 - f_i^{\mu}$, where C^{μ}, E_h^{μ} are the average energy gaps due to ionic and covalent effects;
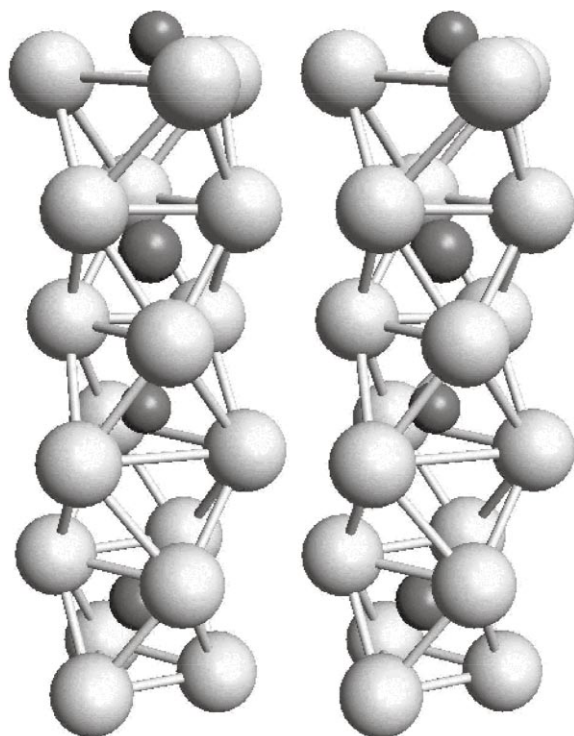d^{μ}: Bond length of the μ-type bonds in Å;

Fig. 1. Stereoscopic view (to be viewed with crossed eyes) of the lithium niobate crystal structure. Light gray: oxygen; small dark spheres: lithium; larger dark spheres: niobium. Oxygen octahedrons and triangles are indicated by sticks.

q^μ: Bond charge of the μth bond;
s: Exponent in the bond force constant (2.48);
$r_c^\mu = 0.35\ r_0^\mu$: Core radius, where $r_0^\mu = d^\mu/2$;
$\rho = (r_A^\mu - r_B^\mu)/(r_A^\mu + r_B^\mu)$: Difference in the atomic sizes, where r_A^μ and r_B^μ are the covalent radii of atoms A and B.

All of the above parameters can be deduced from the detailed chemical bonding structures of all constituent atoms, which are obtained from the corresponding crystallographic structure of the assigned crystal material [24].

3. Results and discussion

The crystal structure of lithium niobate in the ferroelectric room temperature phase is characterized by distorted oxygen octahedra as sketched in Fig. 1. The octahedron centers are occupied by the cations in a stacking sequence … –Li–Nb–☐–Li–Nb–☐–… along the *c*-axis, where ☐ represents a structural vacancy (an empty octahedron) [3]. Nb and Li ions are displaced from the exact center positions along the ferroelectric *c*-axis, thus giving rise to the ferroelectric polarisation. Off-center displacement and distortion of the octahedra cause various different bond lengths for the Nb–O and Li–O bonds, respectively. The principal bond

situation is shown in a stereoscopic view in Fig. 2. Due to the three-fold symmetry, always three equivalent bonds rotationally spaced by 120° exhibit equal lengths. In the calculations, two kinds of Nb–O bonds and two kinds of Li–O bonds are regarded, neglecting the longer ones of the Li–O bonds. When Ta atoms are introduced into the crystal frame, they replace Nb atoms. A corresponding amount of Ta–O bonds instead of Nb–O bonds has to be accounted for in the calculations.

The current work is carried out on the basis of our previous calculations of LN [23,25]. Starting from the detailed crystallographic data of LN and LT, we have calculated corresponding chemical bonding structures of all constituent atoms of LN and LT, respectively. According to the detailed chemical bonding situations of Li, Nb and O atoms, we can calculate chemical bond parameters and linear and second-order NLO properties of all constituent Li–O, Nb–O and Ta–O bonds. The contributions of these constituent chemical bonds are then geometrically summed up yielding the total linear and second-order NLO responses of LN and LT crystals or LNT-type mixed crystals. For the calculation of the linear optical response of LNT, only an isotropic approximation is used yielding the ordinary index of refraction. This is justified by the fact that the birefringence of LN and LT is in the order of 2 and 0.2%, respectively. Effects of this magnitude are beyond the possibilities of the method applied. As a further approximation, we assume in all calculations that length and orientation of all bonds in the mixed crystals is the same as in the respective pure crystals.

We carried out our calculations for crystal compositions of $LiNb_{1-y}Ta_yO_3$ for which experimental values of the refractive indices already have been reported [26], namely for crystals with $y = 0.81$, 0.92, and 0.97. The final values are summarized in Table 1 together with the values for the pure crystals lithium niobate and lithium tantalate, which have a good agreement with the experimental data for NLO coefficients [23,25].

The calculated results for the refractive index are plotted in Fig. 3, for the three independent tensor coefficients of the nonlinear susceptibility in Fig. 4. Also plotted in Fig. 3 are available experimental data for the refractive indices. As is evident from both plots, the dependence on the tantalum content is linear in a very good approximation. The lines plotted in both figures are linear fits to the calculated data. This supports our recent work where we had shown that often a linear correlation between dielectric properties and constituent atoms in crystals with similar structure exists [27].

From the linear fits, the numerical dependence of the dielectric properties on the Ta content y in $LiNb_{1-y}Ta_yO_3$ can be derived to be

$$n_0 = 2.23 - 0.19y \tag{3}$$
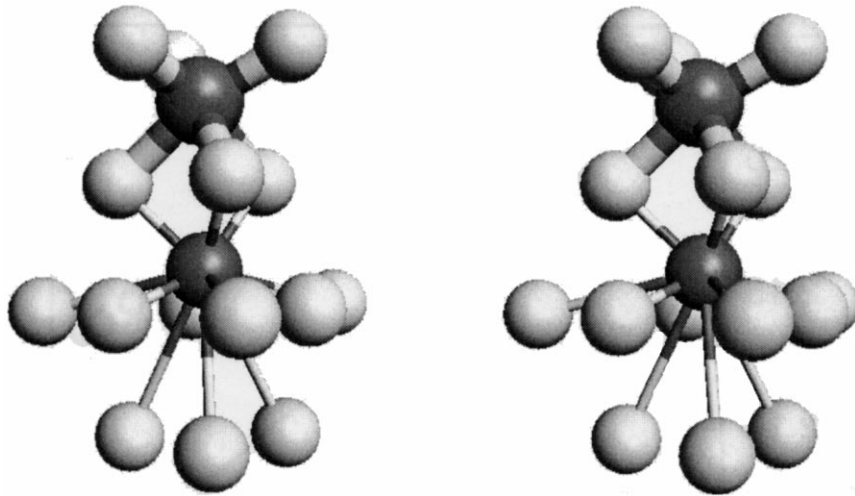
$$d_{22} = 2.72 - 1.08y \tag{4}$$

Fig. 2. Stereoscopic view (to be viewed with crossed eyes) of the bonding topography around niobium (large dark) and lithium ions (small dark) in lithium niobate. Light gray: oxygen ions.

$$d_{31} = -4.94 + 2.21y \qquad (5)$$

$$d_{33} = -25.3 + 9.27y. \qquad (6)$$

Included in both plots are corresponding data for non-stoichiometric lithium niobate where Nb ions replace Li ions up to a certain amount [23]. As can be concluded from the plotted data, the effect of this replacement on the dielectric susceptibilities is remarkably stronger than the effect of the Nb/Ta replacement. This indicates that in the lithium niobate lattice Li sites are much more sensitive to any sort of doping than Nb sites. Two factors are responsible for this matter. When Li is replaced by Nb, four additional Li vacancies are formed, reducing the

dielectric response. Further, the oxygen triangle near the Li site is the largest of all oxygen triangles in the lithium niobate lattice (Fig. 1, thus can be distorted most easily).

4. Conclusion

From the constituent chemical bond viewpoint of crystal materials, we have studied the effect of replacing Nb by Ta cations in lithium niobate crystals on their dielectric properties. Refractive indices and second-order NLO susceptibilities of the $LiNb_{1-y}Ta_yO_3$ type mixed single crystals with $y = 0.00$, 0.81, 0.92, 0.97, and 1.00, at 1.064 μm were
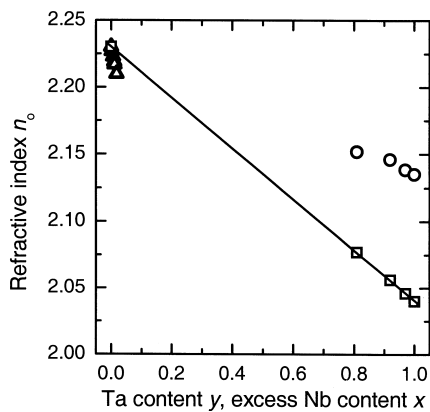

Fig. 3. Refractive index n_0 of lithium niobate tantalate $LiNb_{1-y}Ta_yO_3$ (squares: calculated, circles: experimental) and nonstoichiometric lithium niobate $Li_{1-5x}Nb_{1+x}O_3$ (triangles) as a function of Ta content y or excess Nb content x. The solid line is a linear fit to the calculated data.
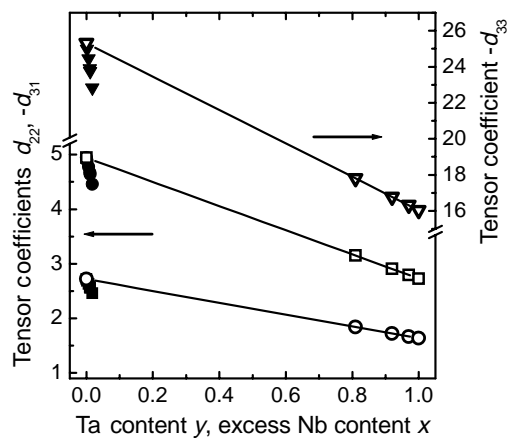

Fig. 4. Tensor coefficients of the nonlinear susceptibility for lithium niobate tantalate $LiNb_{1-y}Ta_yO_3$ (open markers) and nonstoichiometric lithium niobate $Li_{1-5x}Nb_{1+x}O_3$ (filled markers) as a function of Ta content y or excess Nb content x. Circles: d_{22}, squares: d_{31}, triangles: d_{33}. The solid lines are linear fits to the calculated data.

calculated. The present work shows that the dielectric responses of lithium niobate–tantalate decrease approximately linearly with increasing Ta content. A comparison with corresponding data for nonstoichiometric, Li-deficient lithium niobate shows that replacing Li cations has a considerably stronger effect on the dielectric properties. Obviously, lithium sites are the more sensitive lattice sites affecting the dielectric properties of lithium niobate. Therefore, the dielectric properties should be modified more strongly by introducing dopants into lithium sites.

Acknowledgements

References

[1] A. Räuber, in: E. Kaldis (Ed.), Current Topics in Materials Sciences, North Holland, Amsterdam, 1978.

[2] E. Krätzig, O.F. Schirmer, in: P. Günter, J.P. Huignard (Eds.), Photorefractive Materials and their Applications, Springer, Berlin, 1988.

[3] S.C. Abrahams, P. Marsh, Acta Cryst. B 42 (1986) 61.

[4] H. Boysen, F. Altorfer, Acta Cryst. B 50 (1994) 405.

[5] G. Malovichko, V. Grachev, O. Schirmer, Appl. Phys. B 68 (1999) 785.

[6] F.P. Safaryan, R.S. Feigelson, A.M. Petrosyan, J. Appl. Phys. 85 (1999) 8079.

[7] H. Guenther, R. Macfarlane, Y. Furukawa, K. Kitamura, R. Neurgaonkar, Appl. Optics 37 (1998) 7611–7623.

[8] A. Adibi, K. Buse, D. Psaltis, Appl. Phys. Lett. 74 (1999) 3767–3769.

[9] G.W. Baxter, Y. He, B.J. Orr, Appl. Phys. B—Lasers and Optics 67 (1998) 753–756.

[10] H.M. Kretschmann, G. Huber, R.G. Batchko, J.P. Meyn, M.M. Fejer, R.L. Byer, Laser Phys. 9 (1999) 293–298.

[11] D. Hofmann, G. Schreiber, C. Haase, H. Herrmann, W. Grundkotter, R. Ricken, W. Sohler, Optics Lett. 24 (1999) 896–898.

[12] R.C. Miller, W.A. Nordland, Phys. Rev. B 2 (1970) 4896.

[13] G.L. Tangonan, M.K. Barnoski, J.F. Lotspeich, A. Lee, Appl. Phys. Lett. 30 (1977) 238.

[14] J. Koskela, J.V. Knuuttila, P.T. Tikka, C.S. Hartmann, V.P. Plessky, M.M. Appl, Appl. Phys. Lett. 75 (1999) 2683–2685.

[15] J. Imbrock, S. Wevering, K. Buse, E. Kratzig, J. Opt. Soc. Am. B—Optical Phys. 16 (1999) 1392–1397.

[16] Y. Furukawa, K. Kitamura, K. Niwa, H. Hatano, P. Bernasconi, G. P, Gunter, Jpn. J. Appl. Phys. Part 1—Regular Papers Short Notes and Review Papers 38 (1999) 1816–1819.

[17] S.M. Kostritskii, D. Kip, Phys. Status Solidi A—Appl. Res. 169 (1998) 171–180.

[18] D. Kip, Appl. Phys. B—Lasers and Optics 67 (1998) 131–150.

[19] V. Wong, M.C. Gupta, J. Appl. Phys. 84 (1998) 6513–6518.

[20] G.J. Friel, R.S. Conroy, A.J. Kemp, B.D. Sinclair, J.M. Ley, Appl. Phys. B—Lasers and Optics 67 (1998) 267–270.

[21] A. Lorenzo, H. Jaffrezic, B. Roux, G. Boulon, J. Garcia-Sole, Appl. Phys. Lett. 67 (1995) 3735.

[22] U. Schlarb, K. Betzler, Phys. Rev. 50 (1994) 751.

[23] D. Xue, S. Zhang, J. Phys. Condens. Matter 9 (1997) 7515.

[24] D. Xue, S. Zhang, Physica B 262 (1999) 78.

[25] D. Xue, S. Zhang, Phil. Mag. B 78 (1998) 29.

[26] F. Shimura, J. Cryst. Growth 42 (1977) 579.

[27] D. Xue, K. Betzler, H. Hesse, D. Lammers, Phys. Status Solidi (b) 216 (1999) R7.